Modelling non-perturbative corrections to heavy-quark fragmentation

Giancarlo Ferrera

ferrera@fi.infn.it

Università di Firenze

Based on:

U. Aglietti, G. Corcella and G. F., Nucl. Phys. B (2007) [hep-ph/0610035]

G. Corcella and G. F., JHEP (2007) [0706.2357 [hep-ph]]

Outline

Heavy-quark fragmentation

$$e^+e^- \to V(Q) \to H_h + X;$$
$$V = Z^0, \gamma^*, \Upsilon(4s); \quad h = b, c$$
$$m_V, m_h \gg \Lambda_{QCD}$$

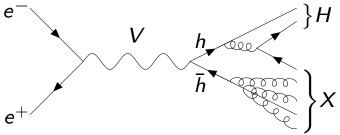

Heavy-quark energy distribution factorizes as [Mele,Nason (91), Cacciari,Catani (01)]:

$$\frac{1}{\sigma}\frac{d\sigma}{dx_h}(x_h;Q^2,m_h^2) = C(x_h;Q^2,\mu_F^2) \otimes E(x_h;\mu_F^2,\mu_{0F}^2) \otimes D^{ini}(x_h;\mu_{0F}^2,m_h^2)$$

where $x_h = 2\,\frac{E_h}{m_V}$;

Perturbative fixed-order expansion feasible but large perturbative terms ($\Rightarrow$ resum) and non-perturbative corrections ($\Rightarrow$ modelize).

Heavy-quark fragmentation

$$e^+e^- \rightarrow V(Q) \rightarrow H_h + X;$$
$$V = Z^0, \gamma^*, \Upsilon(4s); \quad h = b, c$$
$$m_V, m_h \gg \Lambda_{QCD}$$

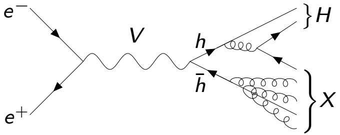

Heavy-quark energy distribution factorizes as [Mele,Nason (91), Cacciari,Catani (01)]:

$$\frac{1}{\sigma}\frac{d\sigma}{dx_h}(x_h;Q^2,m_h^2) = C(x_h;Q^2,\mu_F^2) \otimes E(x_h;\mu_F^2,\mu_{0F}^2) \otimes D^{ini}(x_h;\mu_{0F}^2,m_h^2)$$

where $x_h = 2\,\frac{E_h}{m_V}$;

Perturbative fixed-order expansion feasible but large perturbative terms ($\Rightarrow$ resum) and non-perturbative corrections ($\Rightarrow$ modelize).

Heavy-quark fragmentation

$$e^+e^- \;\to\; V(Q) \;\to\; H_h \,+\, X;$$
$$V = Z^0, \gamma^*, \Upsilon(4s); \quad h = b, c$$
$$m_V, m_h \gg \Lambda_{QCD}$$

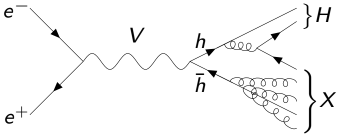

Heavy-quark energy distribution factorizes as [Mele,Nason (91), Cacciari,Catani (01)]:

$$\frac{1}{\sigma}\frac{d\sigma}{dx_h}(x_h;Q^2,m_h^2) = C(x_h;Q^2,\mu_F^2) \otimes E(x_h;\mu_F^2,\mu_{0F}^2) \otimes D^{ini}(x_h;\mu_{0F}^2,m_h^2)$$

where $x_h = 2\,\frac{E_h}{m_V}$;

Perturbative fixed-order expansion feasible but large perturbative terms ($\Rightarrow$ resum) and non-perturbative corrections ($\Rightarrow$ modelize).

- Collinear emission of partons with transverse momenta between $m_h^2 \leq k_\perp^2 \leq m_V^2$ give rise to large logaritmic terms:

$$\alpha_S^n \ln^k \frac{m_V^2}{m_h^2} \qquad (n = 1, 2, \cdots, \infty \quad k = 1, 2, \cdots, n),$$

  which we have resummed using the Altarelli–Parisi (DGLAP) formalism at NLL in $E(x_h;\mu_F^2,\mu_{0F}^2)$.

- In the threshold region ($x_h = 2\frac{E_h}{m_V} \to 1$), soft and/or collinear parton emissions give rise to large logarithmic terms:

$$\alpha^n \left[\frac{\ln^k(1-x_h)}{1-x_h}\right]_+ \qquad (n = 1, 2 \cdots, \infty, \; k = 0, 1, 2, \cdots, 2n{-}1),$$

  which we have resummed at NLO+NNLL in $C(x_h;Q^2,\mu_F^2)$ and $D^{ini}(x_h;\mu_{0F}^2,m_h^2)$ [Sterman ('87), Catani & Trentadue ('89)].

- Collinear emission of partons with transverse momenta between $m_h^2 \leq k_\perp^2 \leq m_V^2$ give rise to large logaritmic terms:

$$\alpha_S^n \ln^k \frac{m_V^2}{m_h^2} \qquad (n = 1, 2, \cdots, \infty \quad k = 1, 2, \cdots, n),$$

  which we have resummed using the Altarelli–Parisi (DGLAP) formalism at NLL in $E(x_h;\mu_F^2,\mu_{0F}^2)$.

- In the threshold region ($x_h = 2\,\frac{E_h}{m_V} \to 1$), soft and/or collinear parton emissions give rise to large logarithmic terms:

$$\alpha^n \left[\frac{\ln^k(1-x_h)}{1-x_h}\right]_+ \qquad (n = 1, 2 \cdots, \infty, \; k = 0, 1, 2, \cdots, 2n-1),$$

  which we have resummed at NLO+NNLL in $C(x_h;Q^2,\mu_F^2)$ and $D^{ini}(x_h;\mu_{0F}^2,m_h^2)$ [Sterman ('87), Catani & Trentadue ('89)].

Perturbative resummation

- In the Mellin space the threshold resummed form factor reads [Catani & Cacciari ('01)]:

$$\ln C_N = \int_0^1 dz \frac{z^{N-1}-1}{1-z}\left\{\int_{\mu_F^2}^{m_Z^2(1-z)} \frac{dk_\perp^2}{k_\perp^2} A[\alpha_S(k_\perp^2)] + B[\alpha_S(m_Z^2(1-z))]\right\}$$

$$\ln D_N^{ini} = \int_0^1 dz \frac{z^{N-1}-1}{1-z}\left\{\int_{m_b^2(1-z)^2}^{\mu_{0F}^2} \frac{dk_\perp^2}{k_\perp^2} A[\alpha_S(k_\perp^2)] + D[\alpha_S(m_b^2(1-z)^2)]\right\}$$

$$A(\alpha_S)=\sum_{n=1}^\infty A_n\alpha_S^n, \quad B(\alpha_S)=\sum_{n=1}^\infty B_n\alpha_S^n, \quad D(\alpha_S)=\sum_{n=1}^\infty D_n\alpha_S^n.$$

- When $z \to 1$ the integration in $k_\perp^2$ involves α_S at the Landau pole: it is necessary a prescription, e. g. the Minimal Prescription [Catani, Mangano, Nason & Trentadue ('96)].
- This fact signal a break-down of the perturbation theory and that truly non-perturbative effects come into play.

Perturbative resummation

- In the Mellin space the threshold resummed form factor reads [Catani & Cacciari ('01)]:

$$\ln C_N = \int_0^1 dz \frac{z^{N-1}-1}{1-z}\left\{\int_{\mu_F^2}^{m_Z^2(1-z)} \frac{dk_\perp^2}{k_\perp^2} A[\alpha_S(k_\perp^2)] + B[\alpha_S(m_Z^2(1-z))]\right\}$$

$$\ln D_N^{ini} = \int_0^1 dz \frac{z^{N-1}-1}{1-z}\left\{\int_{m_b^2(1-z)^2}^{\mu_{0F}^2} \frac{dk_\perp^2}{k_\perp^2} A[\alpha_S(k_\perp^2)] + D[\alpha_S(m_b^2(1-z)^2)]\right\}$$

$$A(\alpha_S) = \sum_{n=1}^{\infty} A_n \alpha_S^n, \quad B(\alpha_S) = \sum_{n=1}^{\infty} B_n \alpha_S^n, \quad D(\alpha_S) = \sum_{n=1}^{\infty} D_n \alpha_S^n.$$

- When $z \to 1$ the integration in $k_\perp^2$ involves α_S at the Landau pole: it is necessary a prescription, e. g. the Minimal Prescription [Catani, Mangano, Nason & Trentadue ('96)].
- This fact signal a break-down of the perturbation theory and that truly non-perturbative effects come into play.

Perturbative resummation

- In the Mellin space the threshold resummed form factor reads [Catani & Cacciari ('01)]:

$$\ln C_N = \int_0^1 dz \frac{z^{N-1}-1}{1-z}\left\{\int_{\mu_F^2}^{m_Z^2(1-z)} \frac{dk_\perp^2}{k_\perp^2} A[\alpha_S(k_\perp^2)] + B[\alpha_S(m_Z^2(1-z))]\right\}$$

$$\ln D_N^{ini} = \int_0^1 dz \frac{z^{N-1}-1}{1-z}\left\{\int_{m_b^2(1-z)^2}^{\mu_{0F}^2} \frac{dk_\perp^2}{k_\perp^2} A[\alpha_S(k_\perp^2)] + D[\alpha_S(m_b^2(1-z)^2)]\right\}$$

$$A(\alpha_S) = \sum_{n=1}^{\infty} A_n \alpha_S^n, \quad B(\alpha_S) = \sum_{n=1}^{\infty} B_n \alpha_S^n, \quad D(\alpha_S) = \sum_{n=1}^{\infty} D_n \alpha_S^n.$$

- When $z \to 1$ the integration in $k_\perp^2$ involves α_S at the Landau pole: it is necessary a prescription, e. g. the Minimal Prescription [Catani, Mangano, Nason & Trentadue ('96)].
- This fact signal a break-down of the perturbation theory and that truly non-perturbative effects come into play.

Model for non-perturbative corrections

- Non perturbative corrections cannot be calculated from first principles. They are usually described using phenomenological hadronization models, with free parameters to be fitted to experimental data.

$$D(x_h) = D_{Pt}(x_h, \mu_{0F}^2, m_h^2) \otimes D_{NP}(x_h, \epsilon_1, \cdots, \epsilon_n)$$

$$D_{NP}(x,\epsilon) = \frac{1}{x[1-\frac{1}{x}-\frac{\epsilon}{1-x}]^2}\,, \quad \text{[Peterson et al. ('83)]}$$

$$D_{NP}(x,\epsilon) = x^{\epsilon}(1-x)\,, \quad \text{[Kartvelishvili et al. ('78)]}$$

- Our approach is different, we treat the unphysical Landau pole from the very beginning using the NNLO analytic QCD coupling [Aglietti & Ricciardi ('04)]. This provide us a model for non-perturbative corrections.

Model for non-perturbative corrections

- Non perturbative corrections cannot be calculated from first principles. They are usually described using phenomenological hadronization models, with free parameters to be fitted to experimental data.

$$D(x_h) = D_{Pt}(x_h, \mu_{0F}^2, m_h^2) \otimes D_{NP}(x_h, \epsilon_1, \cdots, \epsilon_n)$$

$$D_{NP}(x, \epsilon) = \frac{1}{x[1 - \frac{1}{x} - \frac{\epsilon}{1-x}]^2}\,, \quad \text{[Peterson et al. ('83)]}$$

$$D_{NP}(x, \epsilon) = x^{\epsilon}(1 - x)\,, \quad \text{[Kartvelishvili et al. ('78)]}$$

- Our approach is different, we treat the unphysical Landau pole from the very beginning using the NNLO analytic QCD coupling [Aglietti & Ricciardi ('04)]. This provide us a model for non-perturbative corrections.

Analytic QCD coupling

- Standard QCD coupling: physical cut at $\mu^2 < 0$ and unphysical pole at $\mu^2 = \Lambda^2_{QCD}$:

$$\alpha_S^{lo}(\mu^2) = \frac{1}{\beta_0 \ln \frac{\mu^2}{\Lambda^2_{QCD}}} \; .$$

- Analytic QCD coupling: same discontinuity along the cut but analytic elsewhere in the complex plane [Shirkov & Solovtsov ('97)]:

$$\bar{\alpha}_S^{lo}(Q^2) = \frac{1}{\beta_0}\left[\frac{1}{\ln Q^2/\Lambda^2_{QCD}} - \frac{\Lambda^2_{QCD}}{Q^2 - \Lambda^2_{QCD}}\right] , \quad LO \quad space-like$$

$$\lim_{Q^2\to 0} \bar{\alpha}_S(Q^2) = \frac{1}{\beta_0} \, , \qquad \lim_{Q^2\to\infty} \bar{\alpha}_S(Q^2) = \lim_{Q^2\to\infty} \alpha_S(Q^2) \; .$$

Analytic QCD coupling

- Standard QCD coupling: physical cut at $\mu^2 < 0$ and unphysical pole at $\mu^2 = \Lambda^2_{QCD}$:

$$\alpha_S^{lo}(\mu^2) = \frac{1}{\beta_0 \ln \frac{\mu^2}{\Lambda^2_{QCD}}} \, .$$

- Analytic QCD coupling: same discontinuity along the cut but analytic elsewhere in the complex plane [Shirkov & Solovtsov ('97)]:

$$\bar{\alpha}_S^{lo}(Q^2) = \frac{1}{\beta_0}\left[\frac{1}{\ln Q^2/\Lambda^2_{QCD}} - \frac{\Lambda^2_{QCD}}{Q^2 - \Lambda^2_{QCD}}\right] \, , \quad LO \quad space-like$$

$$\lim_{Q^2\to 0} \bar{\alpha}_S(Q^2) = \frac{1}{\beta_0} \, , \qquad \lim_{Q^2\to\infty} \bar{\alpha}_S(Q^2) = \lim_{Q^2\to\infty} \alpha_S(Q^2) \, .$$

Analytic QCD coupling

- Standard QCD coupling: physical cut at $\mu^2 < 0$ and unphysical pole at $\mu^2 = \Lambda^2_{QCD}$:

$$\alpha_S^{lo}(\mu^2) = \frac{1}{\beta_0 \ln \frac{\mu^2}{\Lambda^2_{QCD}}} .$$

- Analytic QCD coupling: same discontinuity along the cut but analytic elsewhere in the complex plane [Shirkov & Solovtsov ('97)]:

$$\bar{\alpha}_S^{lo}(Q^2) = \frac{1}{\beta_0}\left[\frac{1}{\ln Q^2/\Lambda^2_{QCD}} - \frac{\Lambda^2_{QCD}}{Q^2 - \Lambda^2_{QCD}}\right] , \quad LO \quad space-like$$

$$\lim_{Q^2\to 0} \bar{\alpha}_S(Q^2) = \frac{1}{\beta_0} , \qquad \lim_{Q^2\to\infty} \bar{\alpha}_S(Q^2) = \lim_{Q^2\to\infty} \alpha_S(Q^2) .$$

- heavy-quark fragmentation is a time-like process: the analytic coupling in the time-like region reads

$$\tilde{\alpha}_S(k_\perp^2) = \frac{i}{2\pi} \int_0^{k_\perp^2} ds \, Disc_s \, \frac{\bar{\alpha}_S(-s)}{s} .$$

- At leading order we have:

$$\tilde{\alpha}_S^{lo}(k_\perp^2) = \frac{1}{\beta_0} \left(\frac{1}{2} - \frac{1}{\pi} \arctan \frac{\ln \frac{k_\perp^2}{\Lambda_{QCD}^2}}{\pi} \right) ,$$

$$\lim_{k_\perp^2 \to 0} \tilde{\alpha}_S(k_\perp^2) = \frac{1}{\beta_0} , \qquad \lim_{k_\perp^2 \to \infty} \tilde{\alpha}_S(k_\perp^2) = \lim_{k_\perp^2 \to \infty} \alpha_S(k_\perp^2) .$$

- On the other hand the standard assumption is

$$\ln \frac{|s|}{\Lambda_{QCD}^2} \gg \pi \quad \Rightarrow \quad \frac{i}{2\pi} \int_0^{k_\perp^2} ds Disc_s \frac{\alpha_S(-s)}{s} \simeq \alpha_S(k_\perp^2).$$

- heavy-quark fragmentation is a time-like process: the analytic coupling in the time-like region reads

$$\tilde{\alpha}_S(k_\perp^2) = \frac{i}{2\pi}\int_0^{k_\perp^2} ds\, Disc_s\, \frac{\bar{\alpha}_S(-s)}{s}.$$

- At leading order we have:

$$\tilde{\alpha}_S^{lo}(k_\perp^2) = \frac{1}{\beta_0}\left(\frac{1}{2} - \frac{1}{\pi}\arctan\frac{\ln\frac{k_\perp^2}{\Lambda_{QCD}^2}}{\pi}\right),$$

$$\lim_{k_\perp^2\to 0}\tilde{\alpha}_S(k_\perp^2) = \frac{1}{\beta_0}, \qquad \lim_{k_\perp^2\to\infty}\tilde{\alpha}_S(k_\perp^2) = \lim_{k_\perp^2\to\infty}\alpha_S(k_\perp^2).$$

- On the other hand the standard assumption is

$$\ln\frac{|s|}{\Lambda_{QCD}^2} \gg \pi \quad\Rightarrow\quad \frac{i}{2\pi}\int_0^{k_\perp^2} ds\, Disc_s\, \frac{\alpha_S(-s)}{s} \simeq \alpha_S(k_\perp^2).$$

- heavy-quark fragmentation is a time-like process: the analytic coupling in the time-like region reads

$$\tilde{\alpha}_S(k_\perp^2) = \frac{i}{2\pi}\int_0^{k_\perp^2} ds\, Disc_s\, \frac{\bar{\alpha}_S(-s)}{s}.$$

- At leading order we have:

$$\tilde{\alpha}_S^{lo}(k_\perp^2) = \frac{1}{\beta_0}\left(\frac{1}{2} - \frac{1}{\pi}\arctan\frac{\ln\frac{k_\perp^2}{\Lambda_{QCD}^2}}{\pi}\right),$$

$$\lim_{k_\perp^2\to 0}\tilde{\alpha}_S(k_\perp^2) = \frac{1}{\beta_0}, \qquad \lim_{k_\perp^2\to\infty}\tilde{\alpha}_S(k_\perp^2) = \lim_{k_\perp^2\to\infty}\alpha_S(k_\perp^2).$$

- On the other hand the standard assumption is

$$\ln\frac{|s|}{\Lambda_{QCD}^2} \gg \pi \quad\Rightarrow\quad \frac{i}{2\pi}\int_0^{k_\perp^2} ds\, Disc_s\, \frac{\alpha_S(-s)}{s} \simeq \alpha_S(k_\perp^2).$$

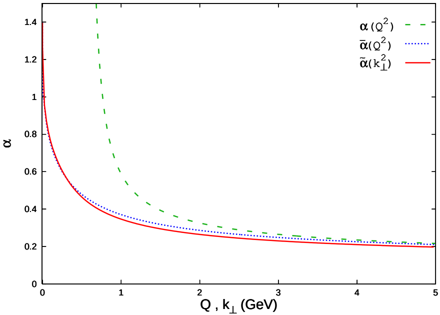

Figure 1: Time-like and space-like analytic couplings compared with the standard one.

We have a modified threshold resummation formula (analogously for C_N and E_N.)

$$\ln D_N^{ini} = \int_0^1 dx \frac{x^{N-1}-1}{1-x} \left\{ \int_{m_b^2(1-x)^2}^{\mu_{0F}^2} \frac{dk_\perp^2}{k_\perp^2} \tilde{A}\left[\tilde{\alpha}_S(k_\perp^2)\right] + \tilde{D}\left[\tilde{\alpha}_S(m_b^2(1-x)^2)\right] \right\}$$

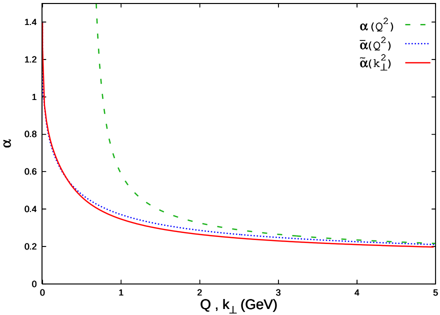

Figure 1: Time-like and space-like analytic couplings compared with the standard one.

We have a modified threshold resummation formula (analogously for C_N and E_N.)

$$\ln D_N^{ini} = \int_0^1 dx \frac{x^{N-1}-1}{1-x} \left\{ \int_{m_b^2(1-x)^2}^{\mu_{0F}^2} \frac{dk_\perp^2}{k_\perp^2} \tilde{A}\,[\tilde{\alpha}_S(k_\perp^2)] + \tilde{D}\,[\tilde{\alpha}_S(m_b^2(1-x)^2)] \right\}$$

Phenomenological Analysis: b-quark fragmentation at the Z^0 peak

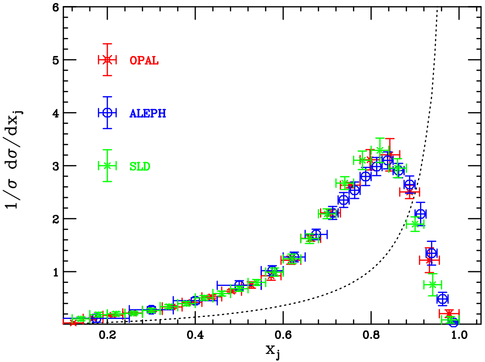

Figure 2: B-hadron spectrum in e^+e^- annihilation at Z^0 peak: prevision of the model compared with experimental data [Aleph ('01), Delphi ('02), SLD ('00)].

Phenomenological Analysis: *b*-quark fragmentation at the Z^0 peak

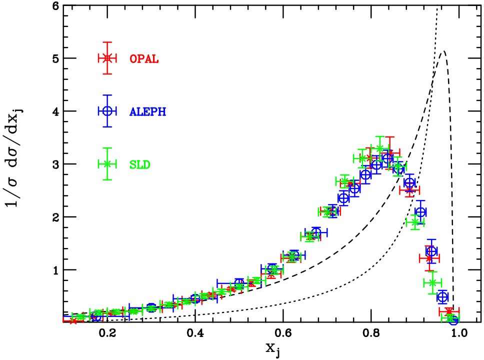

Figure 2: *B*-hadron spectrum in e^+e^- annihilation at Z^0 peak: prevision of the model compared with experimental data [Aleph ('01), Delphi ('02), SLD ('00)].

Phenomenological Analysis: *b*-quark fragmentation at the Z^0 peak

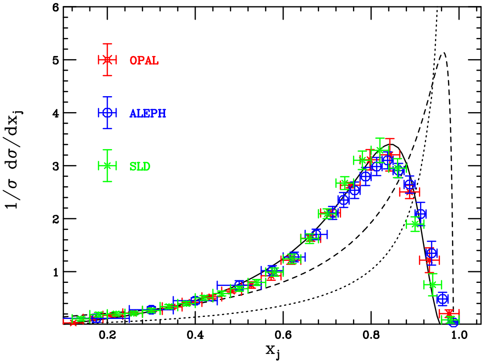

Figure 2: *B*-hadron spectrum in e^+e^- annihilation at Z^0 peak: prevision of the model compared with experimental data [Aleph ('01), Delphi ('02), SLD ('00)].

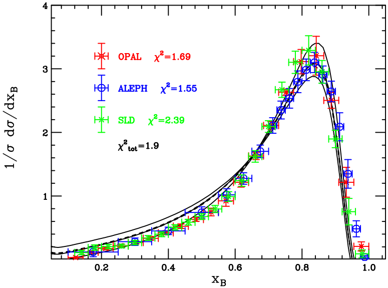

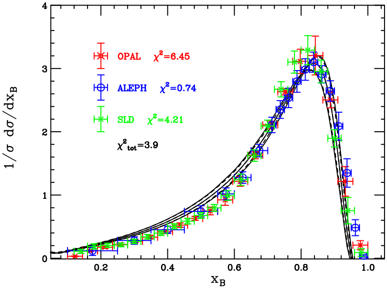

Figure 3: Model dependence on the factorizations scales (left): $\mu_{0F} = m_b/2$, m_b, $2m_b$; $\mu_F = m_Z/2$, m_Z, $2m_Z$ and on $\alpha_S(m_Z)$ and on m_b (right): $\alpha_S(m_Z) = 0.117,\ 0.119,\ 0.121$; $m_b = 4.7,\ 5.0,\ 5.3$ GeV.

	$\langle x\rangle$	$\langle x^2\rangle$	$\langle x^3\rangle$	$\langle x^4\rangle$
e^+e^- data σ_N^B	**0.7153 ± 0.0052**	**0.5401 ± 0.0064**	**0.4236 ± 0.0065**	**0.3406 ± 0.0064**
$[\sigma_N^B]_{\rm th}$	**0.6867 ± 0.0403**	**0.5019 ± 0.0472**	**0.3815 ± 0.0465**	**0.2976 ± 0.0462**
$\delta\sigma_N^B(\mu_R)$	0.0014	0.0011	0.0009	0.0007
$\delta\sigma_N^B(\mu_F)$	0.0066	0.0067	0.0059	0.0051
$\delta\sigma_N^B(\mu_{0R})$	0.0022	0.0028	0.0031	0.0033
$\delta\sigma_N^B(\mu_{0F})$	0.0364	0.0414	0.0398	0.0364
$\delta\sigma_N^B(m_b)$	0.0111	0.0145	0.0153	0.0150
$\delta\sigma_N^B(\bar{m}_b)$	0.0004	0.0005	0.0006	0.0006
$\delta\sigma_N^B(\bar{m}_c)$	0.0003	0.0005	0.0006	0.0006
$\delta\sigma_N^B(\bar{m}_s)$	0.0004	0.0007	0.0008	0.0008
$\delta\sigma_N^B(\alpha_S(m_Z^2))$	0.0113	0.0158	0.0173	0.0176
σ_N^b	0.7734 ± 0.0232	0.6333 ± 0.0311	0.5354 ± 0.0345	0.4617 ± 0.0346

Table 1: Moments σ_N^B from [DELPHI ('02)] and moments $[\sigma_N^B]_{\rm th}$ yielded by our calculation. We quote the uncertainties due to the parameters which enter in the perturbative calculations and compute the theoretical total error. We also present the moments σ_N^b of the standard NLL parton level result.

Charm-quark fragmentation at Z^0 peak

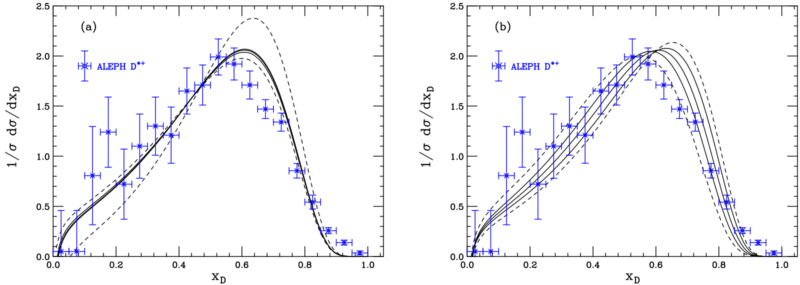

Figure 4: Model dependence on the factorizations scales (left): $\mu_{0F} = m_c/2$, m_c, $2m_c$; $\mu_F = m_Z/2$, m_Z, $2m_Z$ and on $\alpha_S(m_Z)$ and on m_b (right): $\alpha_S(m_Z) = 0.117,\ 0.119,\ 0.121$; $m_b = 1.5,\ 1.8,\ 2.1$ GeV.

Charm-quark fragmentation at $\Upsilon(4s)$ peak

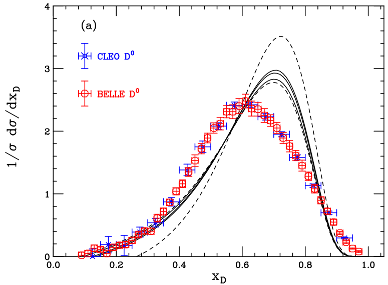

Figure 5: Model dependence on the factorizations scales (left): $\mu_{0F} = m_c/2$, m_c, $2m_c$; $\mu_F = m_Z/2$, m_Z, $2m_Z$ and on $\alpha_S(m_Z)$ and on m_b (right): $\alpha_S(m_Z) = 0.117,\ 0.119,\ 0.121$; $m_b = 1.5,\ 1.8,\ 2.1$ GeV.

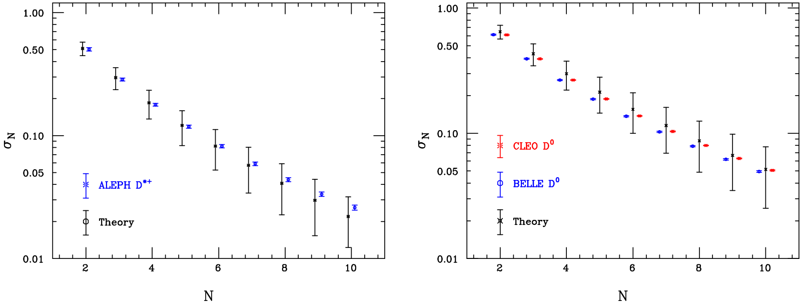

Figure 6: Moments form [Aleph, CLEO, and Belle]compared with model predictions.

Conclusions

- We resummed large logarithm correction to heavy flavour fragmentation up to NNLL matching to the NLO fixed oreder result.
- Using the analytic QCD coupling we develop a model for non-perturbative effects which allow us to describes experimental data in b and c-quark fragmentation without introducing any ad-hoc non-perturbative component. The model works better for processes characterized by an hard scale $Q \sim m_Z$.
  The model was also tested in semi-inclusive B decays.
- Possible future perspectives: perform a complete NNLO+NNLL for heavy flavour fragmentation and use the model to study HERA and Tevatron hadron production data and to make prediction for LHC.

Conclusions

- We resummed large logarithm correction to heavy flavour fragmentation up to NNLL matching to the NLO fixed oreder result.
- Using the analytic QCD coupling we develop a model for non-perturbative effects which allow us to describes experimental data in b and c-quark fragmentation without introducing any ad-hoc non-perturbative component. The model works better for processes characterized by an hard scale $Q \sim m_Z$.
  The model was also tested in semi-inclusive B decays.
- Possible future perspectives: perform a complete NNLO+NNLL for heavy flavour fragmentation and use the model to study HERA and Tevatron hadron production data and to make prediction for LHC.

Conclusions

- We resummed large logarithm correction to heavy flavour fragmentation up to NNLL matching to the NLO fixed oreder result.
- Using the analytic QCD coupling we develop a model for non-perturbative effects which allow us to describes experimental data in b and c-quark fragmentation without introducing any ad-hoc non-perturbative component. The model works better for processes characterized by an hard scale $Q \sim m_Z$.
  The model was also tested in semi-inclusive B decays.
- Possible future perspectives: perform a complete NNLO+NNLL for heavy flavour fragmentation and use the model to study HERA and Tevatron hadron production data and to make prediction for LHC.

Back-up Slides

Comparison with DMW model

- Since the time-like coupling is regular for any value of $k_\perp$, we can compute the average of the coupling

$$\alpha_0 = \frac{1}{\mu_I} \int_0^{\mu_I} \tilde{\alpha}_S(k_\perp^2)\, dk_\perp ,$$

which is a free parameter to be determined with a fit to experimental data [Dokshitzer, Marchesini & Webber ('95)].

- Assuming $\alpha_S(m_b) = 0.22$, $n_f = 3$ and $\mu_I = 2\ GeV$, we obtain at leading order with the time-like coupling:

$$\alpha_0 \simeq 0.44.$$

- The fitted value from shape variable in e^+e^- data is around 0.45, not distant from our estimate.

Comparison with DMW model

- Since the time-like coupling is regular for any value of $k_\perp$, we can compute the average of the coupling

$$\alpha_0 = \frac{1}{\mu_I} \int_0^{\mu_I} \tilde{\alpha}_S(k_\perp^2)\, dk_\perp ,$$

which is a free parameter to be determined with a fit to experimental data [Dokshitzer, Marchesini & Webber ('95)].

- Assuming $\alpha_S(m_b) = 0.22$, $n_f = 3$ and $\mu_I = 2\ GeV$, we obtain at leading order with the time-like coupling:

$$\alpha_0 \simeq 0.44.$$

- The fitted value from shape variable in e^+e^- data is around 0.45, not distant from our estimate.

Comparison with DMW model

- Since the time-like coupling is regular for any value of $k_\perp$, we can compute the average of the coupling

$$\alpha_0 = \frac{1}{\mu_I} \int_0^{\mu_I} \tilde{\alpha}_S(k_\perp^2)\, dk_\perp,$$

which is a free parameter to be determined with a fit to experimental data [Dokshitzer, Marchesini & Webber ('95)].

- Assuming $\alpha_S(m_b) = 0.22$, $n_f = 3$ and $\mu_I = 2\ GeV$, we obtain at leading order with the time-like coupling:

$$\alpha_0 \simeq 0.44.$$

- The fitted value from shape variable in e^+e^- data is around 0.45, not distant from our estimate.